The Transonic Multifoil Augmentor Wing

J.E. Farbridge*
The de Havilland Aircraft of Canada, Ltd., Downsview, Ontario, Canada
and
Ronald C. Smith†
NASA Ames Research Center, Moffett Field, Calif.

The paper describes the development of a thick ($t/c = 0.18$) transonic, multifoil, blown augmentor-wing section and discusses the results of a series of wind-tunnel tests on the configuration. The results show that the blown multifoil section enjoys two advantages over a conventional unblown single-foil supercritical section of the same overall thickness-chord ratio: 1) "effective" drag reduced by blowing, and 2) increased drag rise Mach number ($M_D = 0.75$); they also demonstrate that augmentor blowing improves the buffet boundaries of the section. Thus, overall, it has been shown that the augmentor flap configuration is capable of extending the speed range of a jet transport aircraft to the very low approach speeds required by STOL aircraft [as demonstrated by the NASA/DITC (Canadian Department of Industry Trade and Commerce) augmentor-wing STOL research aircraft] and also to the high subsonic speed required for cruise, where it is shown to be competitive with the plain supercritical airfoil.

Introduction

THE augmentor-wing concept (Fig. 1) was conceived over 16 years ago by de Havilland Aircraft of Canada as a means of powerplant/aerodynamic integration whereby STOL lift coefficients could be developed on a turbofan aircraft with the least penalty in installed thrust-to-weight ratio. The concept has proceeded steadily through the years sponsored jointly by the U.S. and Canadian governments. Many small- and large-scale, low-speed, wind-tunnel tests were performed which, when complemented by design studies and simulator programs, led to the augmentor-wing jet STOL research aircraft (Fig. 2) which is presently in the fifth year of a successful research flying program at NASA Ames.

The concept has seen many system simplifications and performance improvements in the course of developing the low-speed STOL characteristics. Also, it was recognized early in the development process that a considerable simplification would result if the augmentor foils could remain open at all times, that is, even at transonic cruise speeds. Four aerodynamic areas were identified where the multifoil transonic airfoil concept would require careful study: drag level of the unblown multifoil airfoil, drag rise Mach number, buffet boundary, and thrust augmentation of the blown foil at high speed (which might fall to values appreciably less than unity).

It is believed that the concept is original in that no other work has been found which considers the characteristics of a transonic triple airfoil. Also, an exhaustive search of the literature has yielded no reference documenting the influence of very high secondary flow speeds on the thrust augmentation of either axial augmentor, or two-dimensional augmentors such as used on the augmentor-wing concept.

A joint program to investigate the characteristics of a blown, multifoil, augmentor-wing section was initiated in 1972 and sponsored jointly by NASA Ames and the Canadian Department of National Defence. The present paper is a summary of the results to date.

Presented as Paper 77-606 at the AIAA/NASA Ames V/STOL Conference, Palo Alto, Calif., June 6-8, 1977; submitted July 13, 1977; revision received May 17, 1978.

Index categories: Aerodynamics, Transonic Flow.

*Senior Research Engineer.

†Research Scientist and Project Manager.

Potential Advantages of the Multifoil Augmentor Wing for Transonic Cruise Speeds

The potential advantages from keeping the augmentor open, over the entire speed range of the aircraft, include the following.

Systems

1) Simplification of the augmentor flap operating system: no longer any requirement to close the augmentor (Fig. 3).

2) Elimination of the flow diverting system: no longer a requirement to divert the engine air flowing through the wing ducts at low aircraft speeds to cruise nozzles at high speeds (Fig. 3).

Structures

1) Easing of the depth constraint on flap structure: no longer a constraint on flap segment thickness-chords through the need to close these segments into a given high-speed airfoil contour.

2) No requirement for separate cruise nozzles to divert the wing blowing air for cruise.

3) Potential for thicker wings leading to a reduction in structural weight and increased torsional stiffness, permitting, in turn, higher aspect ratio wings for high-speed flight.

Aerodynamics

1) Removal of the boundary layer over 60% of the wing chord, i.e. from both the upper and lower main foil surfaces, and its ingestion into the augmentor; thereby increasing the propulsion efficiency.

2) The beneficial effect of a nonuniform entry velocity distribution of the secondary flow on the performance of the ejector (see Von Karman's fundamental theory[1]).

3) Shock induced boundary-layer separations on the shrouds should be inhibited for the following reasons: a) new, high-energy, boundary layers starting at the leading edges of the upper and lower augmentor segments; b) these segments are only 30-35% of the length of the overall airfoil chord and relatively thinner than the main foil; and c) the adverse effects of angle of attack should have little effect on these boundary layers.

4) The boundary layers on the upper and lower airfoil surfaces of the wing are separated by a jet, thus the two layers will not influence each other aerodynamically. Sudden

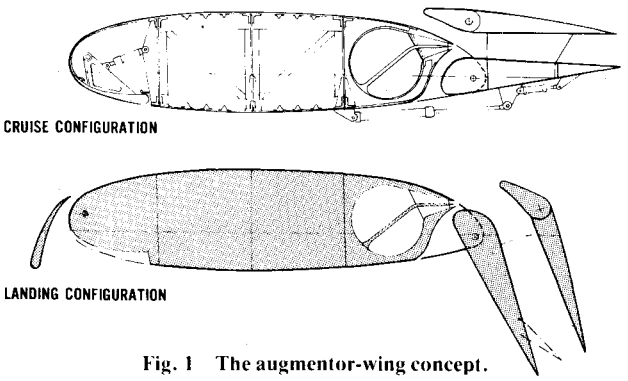

Fig. 1 The augmentor-wing concept.

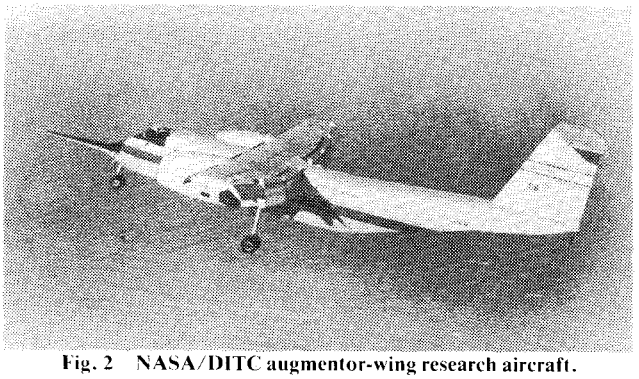

Fig. 2 NASA/DITC augmentor-wing research aircraft.

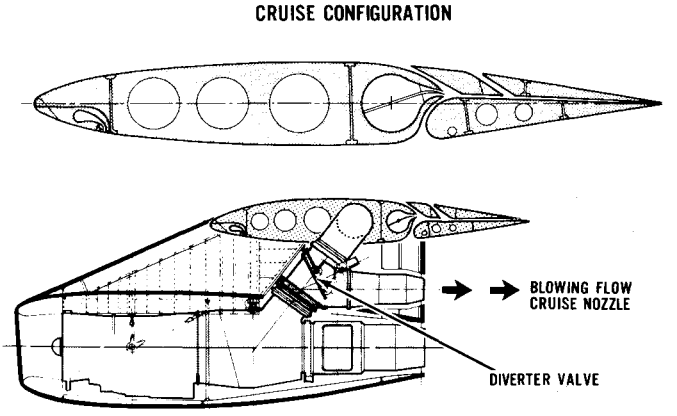

Fig. 3 Augmentor-wing section cruise configuration.

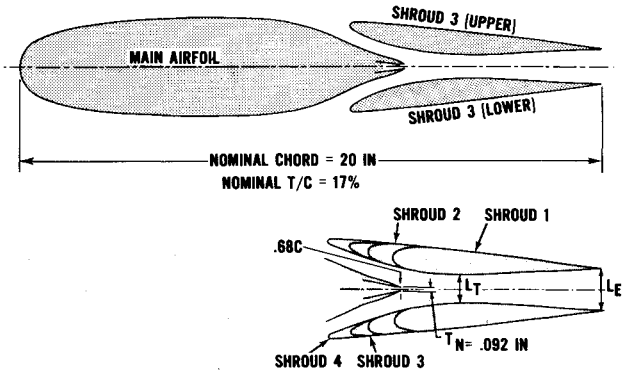

Fig. 4 Symmetric augmentor model cross section with family of shrouds tested.

relative movements in the upper and lower shock positions at shock separation, due to the influence filtering round the trailing edge (giving rise to the condition known as "buffet") will be reduced if not removed, thereby increasing the Mach number at which the onset of buffet occurs.

5) The augmentor flap can be deflected to camber the airfoil and load the rear section of the foil. For a given C_L, therefore, the load near the leading edge of the foil can be reduced to improve the drag rise Mach number. The same mechanism would permit trimming the airfoil for off-design cruising conditions.

In combination, these advantages could lead to lower structural weight, increased aspect ratio, high subsonic drag rise Mach number, and the ability to optimize the airfoil configuration at off-design cruise speeds. In turn, these factors will improve the specific air range of the aircraft and reduce the fuel required for a given mission.

Areas of particular concern at the time the research was proposed were 1) the drag level of the multifoil combination, (since the increased surface area of the configuration will certainly increase the skin friction), 2) the possibility of a net loss in augmentation, rather than a gain, 3) the drag rise Mach number of the multifoil combination, and 4) the buffet boundary of the very thick main foil.

Outline of the Test Program and Theoretical Approach

The high-speed augmentor program began with a low-speed two-dimensional wind-tunnel test in the NAE 6×9-ft low-speed wind tunnel at Ottawa. This test was to provide some bounds to the multiplicity of parameters available for optimization, such as augmentor throat width, diffuser area ratio, intake widths, and multiple foil aerodynamics, beyond the usual sectional parameters of thickness, camber, and angle of attack. A configuration that was symmetric about the chord line was selected (Fig. 4) to assess the various augmentor parameters without the complication of lift or camber effects. Drag was measured directly on an external wind-tunnel balance and wake-rake measurements were taken to correlate the two methods (the following tests in the high speed, pressurized, wind tunnel would rely on wake-rake measurement of drag). Flight values of freestream velocity to jet velocity ratio (V_∞/V_j) and typical high-speed blowing coefficients (C_j) were simulated in this low-speed test, but could only be achieved by reducing the jet supply pressure to quite low values. Also, Mach and Reynolds numbers were well below cruising values, with a maximum Mach number $M_\infty = 0.33$ and maximum Reynolds number $R_e = 3.0 \times 10^6$. Nevertheless, the test showed good collapse of thrust variation with speed for all nozzle pressure ratios when the data were plotted against V_∞/V_j (Fig. 10). Also, it was shown that experimental values of surface pressure could be predicted using a theoretical approach based upon the Douglas-Neumann multifoil program in conjunction with boundary-layer estimates.

The first high-speed test in the NAE, Ottawa, trisonic 5-ft×5-ft pressurized wind tunnel (with its two-dimensional transonic insert) tested the same symmetrical section as the low-speed tests to true flight Mach and Reynolds numbers; $M_\infty = 0.7$, $R_e = 20 \times 10^6$. In addition, with the theoretical program modified by compressible flow corrections due to Prandtl-Glauert and Kuchemann-Weber, the theory was used to develop some thicker and cambered shroud configurations (Fig. 5) which were also tested.

The theoretical approach, however, indicated that the symmetrical configuration could experience premature separation at relatively low Mach numbers and well forward on the main foil. At the same time, though, the method showed that contours could be developed to delay separation to much higher Mach numbers. In particular, the method indicated that asymmetric configurations could be considered (Fig. 6), these contours being more representative of the high-lift STOL configurations of the augmentor-wing flight research aircraft.

The second high-speed model, with an asymmetric main foil configuration, when tested performed sensibly, as an-

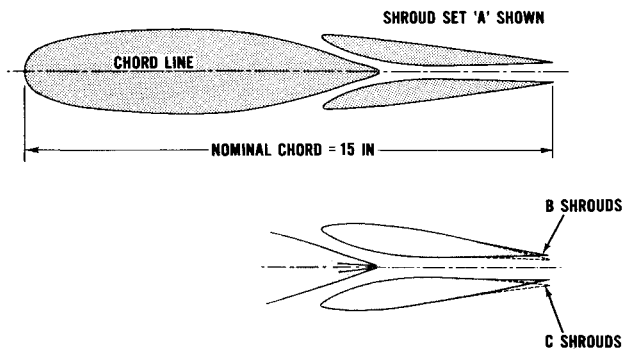

Fig. 5 Section through symmetric augmentor model with different shrouds tested.

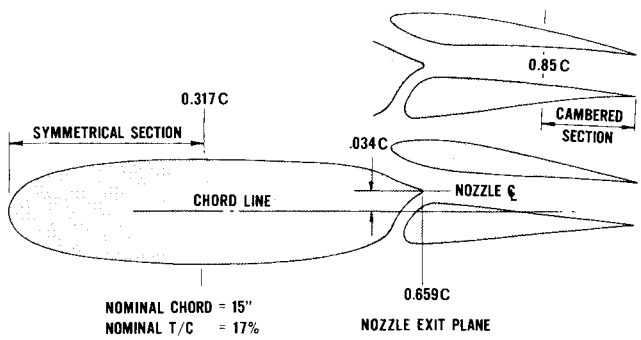

Fig. 6 Section through asymmetrical augmentor with "straight" and cambered shrouds.

ticipated from the theoretical studies. The test also yielded further empirical data on the influence of blowing on the "thrust-minus-drag" characteristics of the augmentor configurations. The influence of supercritical Mach numbers within the augmentors was also explored.

The growing confidence in the theoretical approach led to the development of a third high-speed configuration which would further improve the external high-speed aerodynamics and reconfirm the internal blowing characteristics. In the process of improving the external aerodynamics, the thickness-chord‡ of this new foil increased from 0.168 to 0.178; however theory indicated that the high-speed characteristics would improve even though the design lift coefficient was also increased at the same time to about $C_L = 0.35$. Figure 7 presents a photograph of the second high-speed model configuration showing the method of mounting the shrouds.

Tunnel Measurements

Measurements in the low-speed wind tunnel included lift, drag, and pitching moment obtained from the tunnel balance system. Pressure distributions around the main foil were recorded and wake-rake defect measurements were also taken to correlate with the direct drag measurements.

In the high-speed tests, lift and pitching moment were measured by the tunnel balance system, and the drag was obtained from a wake-rake; as is usual for test configurations of this kind. The wake-rake technique in the 5-ft × 5-ft trisonic wind tunnel has been carefully developed by the NAE staff, and includes the corrections required for a "blown" configuration to account for the externally supplied blowing mass flow injected into the tunnel flow. This method has been documented in Ref. 2. Because of these corrections, considerable care was required in the accurate measurement of this injected mass flow, and a measurement technique was developed by de Havilland using a perforated plate within the model. This plate was incorporated initially to smooth out any internal flow disturbances and to provide a highly uniform spanwise blowing over the full two-dimensional span, but, as noted, further served as an orifice plate. When calibrated, it provided an accurate measurement of mass flow even under the dynamic transient operation of the blowdown tunnel. Wake-rake traverses were taken simultaneously at four spanwise locations.

‡The chord considered here is the overall chord, main foil plus shrouds.

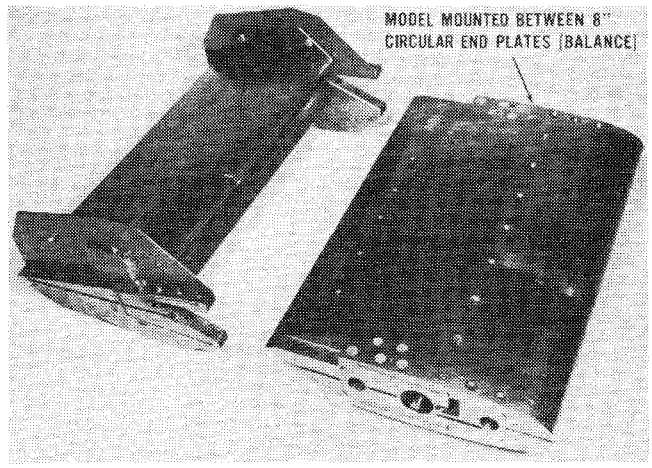

Fig. 7 Asymmetric augmentor model No. 1 shroud and wing assemblies.

$$C_{D_{EFF}} = C_{D_{WRC}} + C_{J_N}$$

WHERE $C_{D_{WRC}}$ IS THE WAKE-RAKE MEASUREMENT CORRECTED FOR THE BLOWING MASS FLOW, i.e.

$$C_{D_{WRC}} = C_{D_0} - \beta C_{J_N}$$

C_{D_0} = THE UNBLOWN PROFILE DRAG COEFFICIENT OF THE SECTION

C_{J_N} = THE MEASURED STATIC NOZZLE THRUST

AND β = THE THRUST COEFFICIENT AUGMENTATION RATIO

β CAN BE RECAST AS

$$\beta = \frac{C_{J_N} + C_{D_0} - C_{D_{EFF}}}{C_{J_N}} = 1 - \frac{\Delta C_{D_{EFF_{C_J}}}}{C_{J_N}}$$

AND $$\Delta C_{D_{EFF_{C_J}}} = C_{D_{EFF}} - C_{D_0} = C_{J_N}(1 - \beta)$$

Fig. 8 Thrust augmentation and effective drag.

Buffetting conditions were detected in the high-speed tunnel at a large increase in the fluctuating normal loads on the rear balance pin. Pressure measurements were taken around the foil surfaces, but it was only during the third high-speed test that a significant number of pressure taps were installed around the shroud foils; this permitted a greater understanding of the influence of blowing on the internal surfaces between the shrouds, on the shroud external surfaces, and on the main foil itself.

To obtain a measure of the influence of augmentor blowing at forward speed it is our general practice to add the static (zero dynamic pressure) blowing thrust of the nozzle, (i.e., without the shrouds) to the wake-rake "drag-minus-thrust" data for the augmentor configuration (Fig. 8). We thus arrive at an "effective" drag for the augmentor section as if the blowing thrust were supplied externally to the configuration. This allows us to make a direct comparison with an unblown profile. If thrust augmentation is realized in the test (i.e., $\phi > 1.0$) then the "effective" drag of the configuration is less than the zero blowing drag and the variation of $C_{D_{\text{eff}}}$ with C_{J_N} provides a direct measure of ϕ.

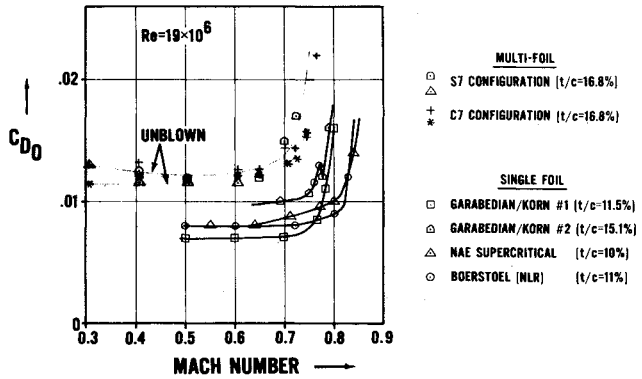

Fig. 9 Unblown profile drag coefficient of the multifoil augmentor compared with single-foil coefficients measured in the same NAE wind tunnel by the same wake-rake methods.

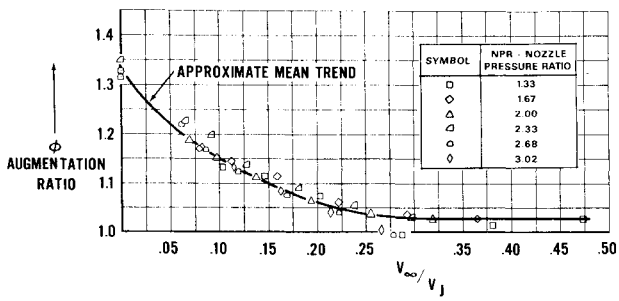

Fig. 10 Correlation of thrust data with velocity ratio.

Multifoil Augmentor-Wing Characteristics

A. Main Foil Boundary-Layer Separation

The large area of separation at the rear of the very thick main foil ($t/c=0.26$), when tested by itself, could generally be eliminated up to transonic Mach numbers by suitable location of the shrouds, even without augmentor blowing.

B. Form Drag (Profile Drag Minus Skin Friction Drag)

The lowest level of profile drag achieved with the best unblown, unseparated, configurations is far less than would be expected from the sum of the three foils individually; even supposing that the main foil, individually, could remain unseparated. In fact, it is only by assuming that the form factor (profile drag/flat-plate skin friction drag) for the main foil alone is essentially unity (and not closer to 2 as might be anticipated for a foil of this thickness-chord), and also assuming that the shroud form factors are not affected by the proximity of the other foils, that the drag of the combination can be predicted theoretically. Figure 9 presents the lowest levels of unblown profile drag achieved in the test series at typical cruise Reynolds numbers of 19×10^6. Profile drag data for several supercritical single foil sections, measured in the same NAE tunnel by the same wake-rake methods, are also presented for comparison.

C. Thrust Augmentation ϕ

Most shroud locations in the high-speed tests, and the best shroud locations in the low-speed test, showed thrust augmentation ratios ϕ greater than unity over the whole speed range tested. These ratios ranged from $\phi=1.03$ to 1.05 at high transonic speeds, corresponding to typical cruise velocity/jet velocity (V_∞/V_j) ratios around 0.6. Figure 10 presents the augmentation data for one configuration of the low-speed tests and shows that, as might be expected from simple ejector theory, the data collapses when plotted against V_∞/V_j.

D. Autonomous External Flow Characteristics

It was observed in all of the studies that, in general, the external flowfield was essentially unchanged by the augmentor blowing. Occasionally, however, very local effects were observed on the external flows in the vicinity of the augmentor intakes if areas of separation existed in the unblown case, and on configurations with a separation bubble located just at the augmentor intake.

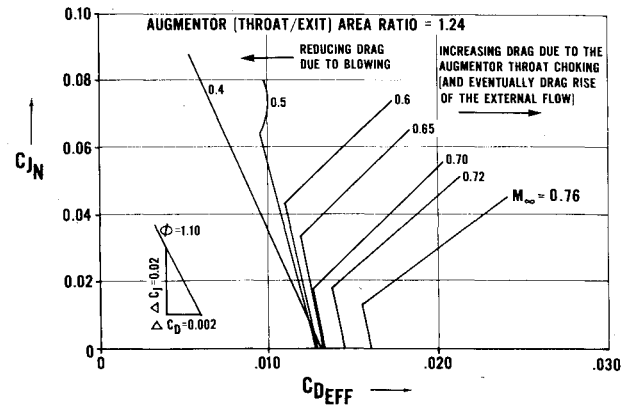

Fig. 11 Influence of large augmentor diffuser ratio at high Mach number (first asymmetric configuration).

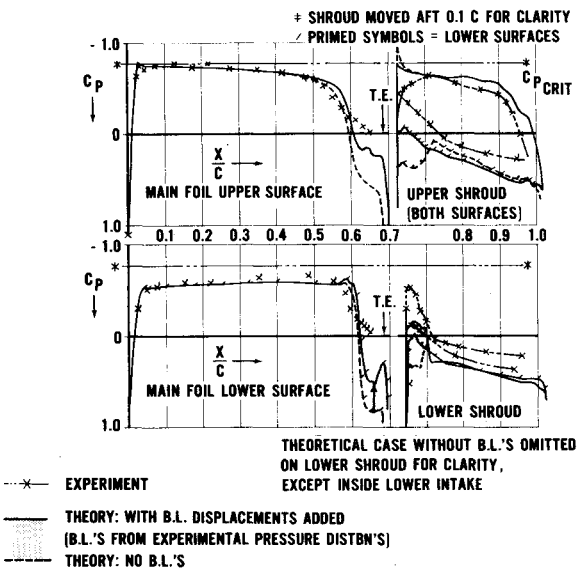

Fig. 12 Correlation of experimental data with theory, $M_\infty=0.702$.

E. Effects of Mach Number on the Internal Characteristics

As the freestream Mach number is increased, the augmentor diffuser area ratio must be reduced to keep the augmentor throat unchoked, particularly with the augmentor blowing. This was anticipated from the theoretical studies, but the significance of the supersonic acceleration of the flow downstream of a choked throat (and the resulting shock in the diffuser) is best demonstrated by Fig. 11. This shows the large increase in effective drag with blowing after the throat chokes for a configuration with a large diffuser area ratio $A_{exit}/A_{throat}=1.24$.

F. Correlation with Theory

One of the most encouraging observations was the ability of the simple homentropic multifoil theory, coupled with estimations of the boundary-layer displacement thicknesses, to predict the pressure distributions around the foils. As details of the theory were refined, satisfactory correlations were achieved up to M_{crit}, which represents the limit of applicability of the method. Figure 12 presents a recent correlation performed with the compressible method. The locations of the boundary-layer separations were also reasonably well predicted, allowing the foils to be developed

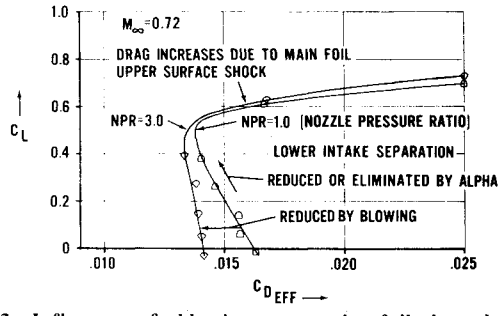

Fig. 13 Influence of blowing on main foil boundary-layer separations.

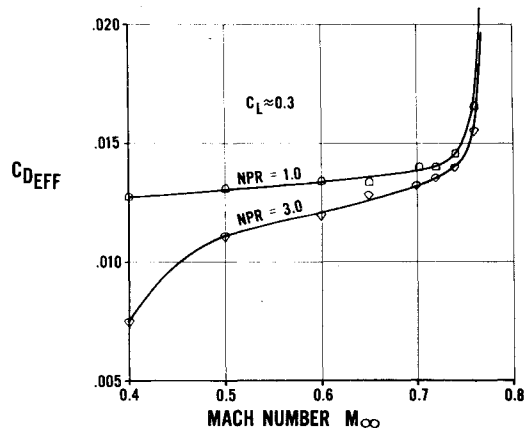

Fig. 14 Variation of unblown (C_{D0}) and blown (C_{Deff}) drag coefficients with Mach number. (Note: the boundary layer on the main foil lower surface was separated with this configuration.)

to high Mach numbers. However, as will be described later, our early main foil boundary-layer displacement thickness predictions proved to be inadequate in areas of strong adverse pressure gradient.

G. Control of Main Foil Separation by Augmentor Blowing

Some difficulty has been experienced in the prediction of boundary-layer thickness in the strong adverse pressure gradients just ahead of the augmentor intakes. In practice the boundary layers were considerably thicker than predicted with the initial boundary-layer estimate, to such an extent that choking occurred in both the upper and lower intakes when the third high-speed configuration was tested. This situation was quickly rectified by direct aft movement of the shroud assembly, but it left the lower shroud in a nonoptimum position in relation to the main foil, and also the shroud contour was by no means optimum. As a consequence, the lower shroud did not control the main foil lower surface boundary-layer separation as anticipated, except at the higher angles of attack as shown by Fig. 13. However, the same figure demonstrates clearly (and confirmed by flow visualization studies) that the augmentor blowing was able to make up for this deficiency and recover some of the drag penalty due to the boundary-layer separation; eventually choking occurred in the intakes, due to the nonoptimum shroud contour, which caused the drag to increase again.

In spite of these difficulties, this third high-speed configuration confirmed the expected improvements—a significant increase in design C_L and an improved drag rise Mach number, $M_D = 0.75$, at this C_L, (Fig. 14). The augmentor *throat* Mach number was held below choking at freestream Mach numbers $M_\infty = 0.78$ and 0.80, up to a blowing pressure ratio of 3.0 (Fig. 15). Also, it should be noted that although the shroud surfaces become supercritical with augmentor blowing, as shown on Fig. 15, these supercritical regions do not extend across the intakes to the main foil (see Fig. 16).

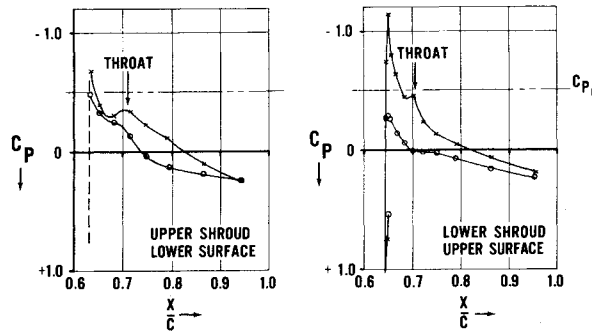

Fig. 15 Internal augmentor pressure distributions at high Mach number. $M_\infty = 0.78$, $C_L = 0.26$, (o)NPR = 1.0, (×)NPR = 3.0. (Note: Supercritical conditions on the shrouds in the intakes to the augmentor do not extend across the intakes; see Fig. 16.)

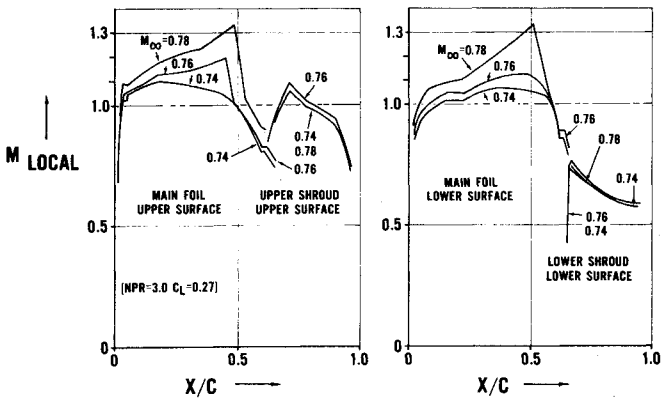

Fig. 16 Variation of external flow local Mach number with freestream Mach number.

A more recent boundary-layer computer program by Bradshaw et al.[3] is presently being used which yields considerably increased boundary-layer displacement thicknesses relative to our original method (by a factor of 2 or 3) in the presence of adverse pressure gradients. Also, the method increases the displacement thicknesses due to the convex curvature of the main foil surfaces into the intakes. Figure 12, in fact, presents a correlation using this more recent method and looking at the pressures within the intakes it would appear we need a still thicker boundary-layer displacement. Bradshaw is presently working on a modified version of his program in which the pressure gradients normal to the airfoil surface are included explicitly, and this could possibly prove to be the final step required. The following sections discuss the remaining topics, drag rise and buffet boundary, and deal only with results from the last high-speed test which gave the best drag divergence and buffet characteristics even though the drag level was somewhat higher than the previous model configuration.

Drag Rise Mach Number

Figure 14 shows that for the 0.178 thickness-chord, two-dimensional, multifoil aerofoil a drag rise Mach number ($dC_D/dM_\infty = 0.1$) of $M_D = 0.75$ has been achieved at a C_L around 0.35 to 0.4. The drag rise is initiated first on the upper surface of the main foil which begins to exhibit supersonic acceleration of the flow beyond the "crest" at a freestream Mach number of $M_\infty = 0.76$ prior to the shocking down (Fig. 16). The figure also shows that the lower surface is still recompressing without shock formation at this Mach number and that the flow around the upper shroud is behaving sensibly as designed, that is "lagging" behind the main foil in its development of supercritical flow.

The pressure distribution data of Fig. 16 show that the main foil lower surface begins to develop supersonic acceleration of

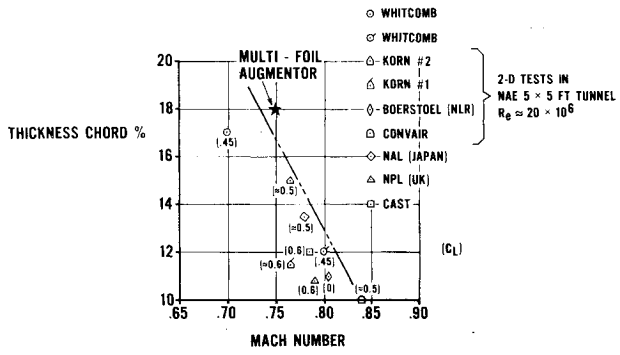

Fig. 17 Published experimental drag rise Mach numbers vs thickness-chord.

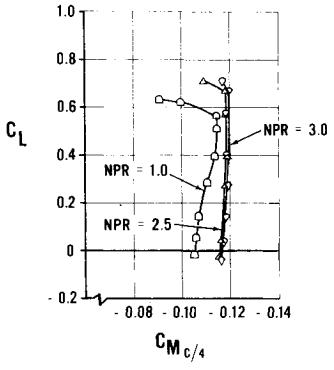

Fig. 18 Pitching moment coefficients for multifoil section, $M_\infty = 0.74$.

the flow at a freestream Mach number around $M_\infty = 0.78$, leading to an increased shock loss. Finally, the figure indicates that the upper shroud still "lags" behind the main foil in the development of supercritical Mach numbers, even at a freestream Mach number of $M_\infty = 0.78$, and seems to be relatively free of significant shock losses. It should be noted that these external pressure distributions are taken at the midspan locations of the two-dimensional section and, at the higher Mach numbers, were sensibly the same blowing on and blowing off. The significance of the blowing, however, was that large three-dimensional effects which occurred at $M_\infty = 0.78$ with blowing off were essentially eliminated by augmentor blowing.

A search of the literature for both experimental[4-6] and theoretical drag rise data for conventional single foils (including some of our own theoretical studies[7]) indicated that a drag rise Mach number of 0.73 to 0.74 might be as high as one could realize for a single foil of $t/c = 0.18$ at $C_L = 0.35$. Values in excess of this have already been demonstrated with the multifoil configuration as shown in Fig. 17 in comparison with other experimental data. This has been achieved for two reasons, firstly the multifoil configuration is loaded further aft due to the upper shroud loading and secondly, the shrouds and the augmentor blowing control separation on the very thick main foil in the region of high-pressure recovery over the rear of the section. The aft loading leads to higher values of nosedown pitching moments (of order $C_m = -0.1$) as shown in Fig. 18.

Buffet Characteristics

The anticipated improvement in the buffet boundary with augmentor blowing was realized (the upper and lower main foil boundary layers being isolated from each other by means of the spanwise jet). These improved buffetting conditions are aided by the fact that the shroud pressure distributions are only slightly influenced by angle of attack. Figure 19 shows the improvement in the lift coefficient at buffet due blowing. Figure 20, which documents the continuous rms normal force on the rear balance pickup pin, shows that the trace with "blowing on" is significantly less noisy than the unblown

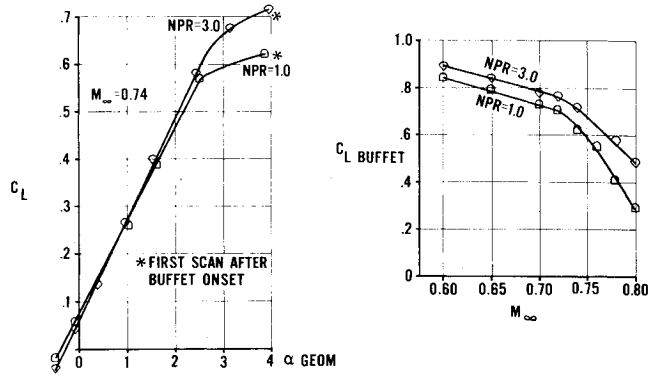

Fig. 19 Variation of lift curve slope and buffet boundaries due to blowing.

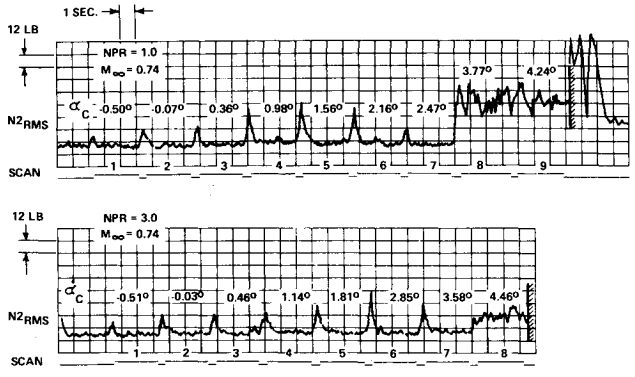

Fig. 20 Influence of blowing on buffet intensity.

configuration at and above the C_L "break-point" used to define buffet. This indicates that buffet, when it does arise, is far less severe with the blowing on. At the highest Mach numbers some of the lift improvement due to augmentor blowing (shown on Fig. 19) may be due to restoration of two-dimensional flow on the model which is mounted between side walls.

Figure 19 shows that the small amount of jet deflection due to the cambered shrouds gives rise to an increase in lift curve slope with blowing (most likely due to the jet flap effect); as well as the increase in the angle of attack for buffet.

Augmentor Effectiveness at High Transonic Speeds

The effectiveness of augmentor blowing at high transonic speeds can be seen clearly from Fig. 21 where the influence of drag creep and drag rise has been removed by referencing the drag to conditions at zero augmentor blowing, $C_{J_N} = 0$. The steady reduction in drag with blowing is very evident at all three, transonic, Mach numbers shown. The data are considered to be correct to within ±5 drag counts and in general scatter about the mean lines for all the configurations shown.

Potential for Improvement

As noted previously the shrouds are relatively free of significant shock losses even at a freestream Mach number of $M_\infty = 0.78$. Thus, it would appear that there is the potential to bring the main foil drag rise up to a Mach number of at least $M_\infty = 0.78$. Changes to the main foil contours in the vicinity of the augmentors intakes will raise the drag rise Mach number and also assist in delaying boundary-layer separation until further aft on the main foil. These changes, coupled with reoptimized shroud leading-edge contours, should lead to intakes which are free from choking at the highest nozzle pressure ratios expected, and to the inhibition of separation of the main foil lower surface boundary layer.

Other "new horizons" can be seen with shorter chord shrouds, to reduce the skin friction drag with the augmentor

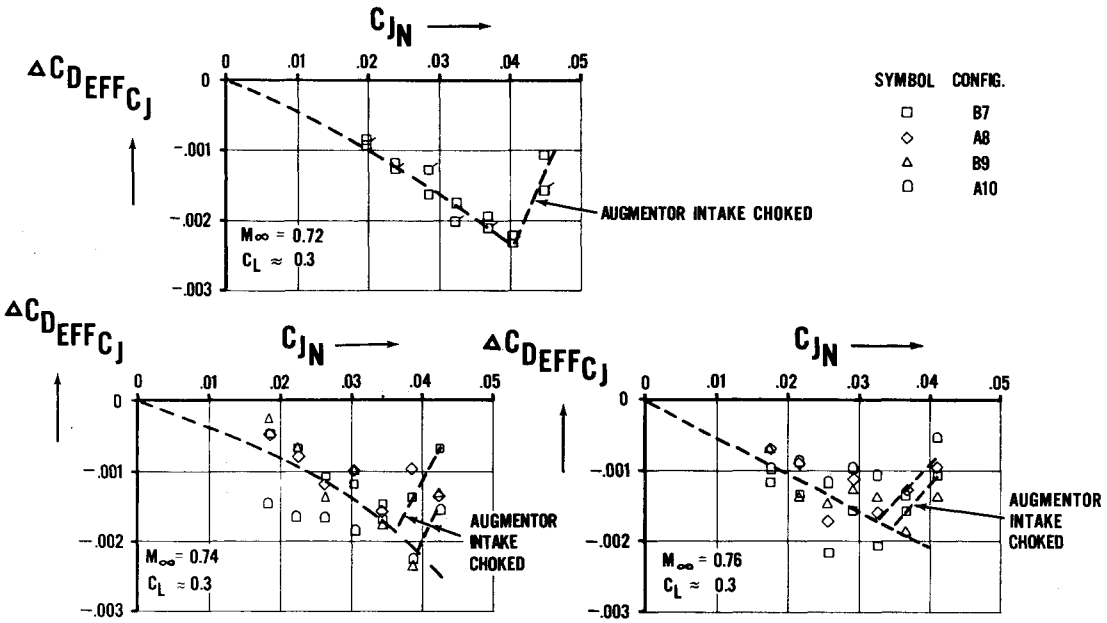

Fig. 21 Reduction of drag due to augmentor blowing.

open. Also, improved levels of thrust augmentation should be realized using segmented, vertically oriented blowing nozzles, which have been successfully demonstrated in our many (unpublished) low-speed studies.

Conclusions

The development of the blown multifoil augmentor-wing for high transonic cruise Mach numbers has led to the following conclusions:

1) A very thick wing can be contemplated since separations towards the rear of the main foil can be controlled both by shroud location and augmentor blowing.

2) Form drag of the main foil section is reduced by presence of the shrouds.

3) Intake momentum reduces augmentation to a relatively constant level at transonic speeds ($\phi = 1.03$ to 1.05).

4) This level of thrust augmentation reduces the "effective" drag of the multifoil configuration appreciably at transonic speeds.

5) At lower Mach numbers, where both the augmentation (ϕ) and the blowing coefficients (C_J) are large, the "effective" profile drag of the section reduces to zero and even negative values.

6) The drag rise Mach number of the multifoil configuration is potentially capable of being significantly higher than that for a single foil.

7) Buffet boundaries are significantly improved by augmentor blowing and the buffetting intensity is also markedly reduced by augmentor blowing. This suggests potential use of the concept for fighter-type aircraft.

Acknowledgments

The work described in this paper is the result of an international collaborative program supported by the Canadian Department of National Defence and the NASA, Ames Research Center. The de Havilland author would like to acknowledge the direction and assistance of D.C. Whittley, Director of Research at de Havilland, and also his colleagues J.L. Harris and D.B. Garland, for their constructive discussions on the results of the wind-tunnel tests. The work of G. Elfstrom, the project monitor for the transonic multifoil augmentor-wing wind-tunnel test program in Ottawa, is also recognized.

References

[1] Von Karman, T., "Theoretical Remarks on Thrust Augmentation," *Contributions to Applied Mechanics*, Reissner Anniversary Volume, 1949.

[2] Peake, D.J., Yoshihara, J., Bowker, J., Mokry, M., and Magnus, R., "Transonic Lift Augmentation of Two-Dimensional Supercritical Aerofoils by means of Aft Camber, Slot Blowing, and Jet Flaps, in High Reynolds Number Flow," presented at 9th Congress International Council of the Aeronautical Sciences, Haifa, Israel, Aug. 25-30, 1974.

[3] Bradshaw, P. and Unsworth, K., "An Improved Fortran Program for the Bradshaw-Ferriss-Atwell Method of Calculating Turbulent Shear Layers," Imperial College Aero Rept. 74-02, Feb. 1974.

[4] Boerstoel, J.W., "Review of Application of Hodograph Theory to Transonic Aerofoil Design and Theoretical and Experimental Analysis of Shock-Free Aerofoils," Symposium Transsonicum II, Gottingen, Sept. 1975.

[5] Kacprzynski, J.J. and Ohman, L.H., "Wind-Tunnel Tests of a Shockless Lifting Airfoil No. 1," National Aeronautical Establishment Rept. No. 5 x 5/0054, Aug. 1971.

[6] Kacprzynski, J.J., "Wind-Tunnel Tests of a Shockless Lifting Airfoil No. 2," National Aeronautical Establishment Rept. No. LTR-HA-5 x 5/0067, Oct. 1973.

[7] Eggleston, B., "An Inverse Method for the Design of Airfoils with Supercritical Flow," SAE Paper 770-450, Business Aircraft Meeting Century II, Wichita, Kansas, 1977.